Supporting Information (SI)

SI Results

POSTN and TWIST1 promote FLS migration *in vivo*. The *in vivo* experiment was performed to confirm the regulation of FLS migration by POSTN or TWIST1. To this end, skin inflammation was induced by subcutaneous injection of complete Freund's adjuvant (CFA) into the right and left back skin of immuno-deficient mice (**Fig. S5*C***). One day after the CFA injection, RA-FLS ($5X10^5$), labeled with fluorescent dyes of NIR 675, were implanted intra-dermally into the mice at a fixed distance (1.2 cm) from the site of the CFA injection (**Fig. S5*C***); Prior to labeling with NIR 675, RA-FLS were transfected with control siRNA, POSTIN siRNA or TWIST1 siRNA for 24 hours. The FLS transfected with siRNA for POSTIN or TWIST1 were implanted into the right back skin exactly opposite to the control siRNA-harboring site on the left. After 5 days of implantation, skin samples were obtained from the FLS-implanted site, CFA-injected site, and between the two **(a**, **c**, and **b** in **Fig. S5*C***, respectively). As seen in **Fig. S5*C***, a cluster of human HLA class I (+) cells, indicating RA-FLS, were highly detectable at all the FLS-implanted sites of the left and right back skin, indicating that human FLS are successfully engrafted in the immuno-deficient mice. Analysis of entire areas between FLS-implanted and CFA-injected site revealed that HLA class I (+) cells were more frequently found in the skin on the left with control siRNA than in those on the right with POSTIN siRNA or TWIST1 siRNA (**Fig. S5*D*** and **S5*E***). The number of fluorescence (+) cells showed similar results (**Fig. S5*D***), suggesting that POSTIN siRNA or TWIST1 siRNA reduces FLS migration toward the CFA-injected site with dermal inflammation. However, RA-FLS were rarely detected at the CFA-injected site, irrespective of siRNA transfection. Overall, these data suggest that POSTIN siRNA or TWIST1 siRNA suppresses FLS migration *in vivo*.

SI Discussion

Implication of POSTN and TWIST1 in the invasion and migration. Given the invasive characteristic of RA-FLS, POSTN and TWIST1 are the intriguing regulatory molecules. POSTN was primarily reported as a matricellular protein, which is secreted into the extracellular environment or matrix. It modulates cell function by interacting with cell-surface receptors, proteases, and other bio-effector molecules, as well as with structural matrix proteins, such as collagens (1). In addition to its extracellular activity, POSTN intracellularly regulates EMT and fibrosis under a wide variety of tumorigenic conditions and tissue repair (2-4). Through POSTN-mediated signaling, tumor cells undergoing fibroblast-like transformation as well as dermal fibroblasts acquire enhanced migratory activity, which could potentially partly determine their invasiveness and profibrotic capacity, respectively (5, 6). TWIST1 belongs to the basic helix-loop-helix (bHLH) transcription-factor family and is well-known for promoting EMT by repressing the expression of E-cadherin, which leads to the disassembly of adherens junctions and pro-migratory potential of various tumor cells and mesenchymal cells (7, 8). Interestingly, POSTN is closely linked to TWIST1 (9), and both of them are activated and play key roles in the organ development process, such as lineage commitment and cellular differentiation (1, 10). In the present study, the involvement of POSTN and TWIST1 in the invasiveness of RA-FLS is novel and has important ramifications for the understanding of the unique aggressive phenotype of RA-FLS and pannus formation.

SI Materials and Methods

Isolation of RA-FLS and SM. FLS were obtained from the synovial tissues of RA or OA patients as described previously (11), and incubated in Dulbecco's modified Eagle's medium (DMEM) supplemented with fetal calf serum (FCS; Gibco, Carlsbad, CA) or with insulin-

transferrin-selenium A (ITSA; Life Technologies, Gaithersburg, MD). The purity of FLS was tested by flow cytometry analysis using phycoerythrin-conjugated anti-CD14 (BD PharMingen, San Diego, CA) and fluorescein isothiocyanate-conjugated anti-Thy-1 (CD90) monoclonal antibody (BD PharMingen). Most cells (>99%) had the surface marker for fibroblasts (Thy-1). Monocytes/macrophages were obtained from mononuclear cells of healthy controls or from the synovial fluid of RA patients using anti-CD14 magnetic beads (Miltenyi Biotec, Auburn, CA), according to the manufacturer's instructions. To induce differentiation into macrophages, peripheral blood monocytes of healthy controls were cultured for 24 hours in RPMI 1640 medium supplemented with 10% FCS in the presence of human M-CSF (20 ng/ml). OA macrophages were freshly isolated from synovial tissues of OA patients using anti-CD14 magnetic beads as described previously (12). The study protocol was approved by the Institutional Review Board of the Catholic Medical Center (XC09TIMI0070). All patients gave written informed consent to the study protocol.

Microarray analysis. In each condition, we prepared total RNA independently from three replicate samples using the RNeasy mini kit (Qiagen, Hilden, Germany) and assessed RNA integrity using Bioanalyzer 2100 (Agilent Technologies, Santa Clara, CA). The RNA integrity number (PRN) was close to 10 for all samples. RNA was then amplified and hybridized to the Illumina HumanHT-12 v4.0 (for FLS) and HumanRef-8 WG-DASL v3 (for synovial macrophages) Expression BeadChip, according to Illumina standard protocols. The probe intensities were normalized using the quantile normalization procedure (13). The data were deposited into the GEO database (GEO accession ID, GSE49604).

Integrative statistical testing for identification of DEGs. For the four comparisons 1)

RA-FLS/OA-FLS, 2) RA-SM/healthy controls, 3) RA-FLS+IL1β/OA-FLS, and 4) RA-FLS+IL1β/OA-FLS+IL1β), we used the integrative statistical method previously reported (14), rather than the conventional t-test and fold-change tests. The t-test can mistakenly identify the genes that have small mean differences, but have further smaller pooled standard deviations, which lead to large t-statistic values close to infinity. On the other hand, the fold-change-based test can mistakenly identify the genes that have large mean differences, but have larger pooled standard deviations with fluctuating expression in replicates under individual conditions. By integrating adjusted the *P*-values from these two tests using Stouffer's method, these false positives can be reduced. See 'Statistical analyses' for the detailed procedures of the integrative statistical method.

Hierarchical clustering of DEGs. From the comparisons of RA-FLS/OA-FLS and RA-SM/healthy controls, we identified a total of 2,376 DEGs. Before clustering these DEGs, they were categorized into the three groups ('Shared', 'FLS-dominant', and 'SM-dominant'). For the DEGs in each group, we further performed a hierarchical clustering using Euclidean distance as the dissimilarity measure and the average linkage method: four clusters (C1-4) for shared DEGs, two clusters (C5-6) for FLS-dominant DEGs, and two clusters (C7-8) for SM-dominant DEGs (*See heat maps* in **Fig. 1B**).

Modular enrichment analysis. To quantitatively assess the contribution of RA-FLS and RA-SM to the individual modules, we calculated a module enrichment score (MES), which was defined as [(number of DEGs within a module) / (total number of genes within the module)] / [(total number of DEGs in the network) / (total number of signature genes)], a modified version of fold enrichment score in the DAVID software (15, 16).

Evaluation of statistical significance of module enrichment scores (MES). To evaluate the significance of a MES in **Fig. S3B**, we performed the following random sampling method: 1) for module *i*, we counted genes in the module among up-regulated genes; 2) we randomly sampled the same number of up-regulated genes from the whole genome, and then counted randomly sampled genes belonging to module *i*; 3) after repeating step 2 100,000 times, we estimated an empirical distribution of 100,000 counts of randomly sampled genes in module *i*; and 4) for the actual count of genes in module *i*, we computed the *P*-value that the actual count can be observed by chance by the one-tailed test using empirical distribution. The same procedure was repeated for all modules in the network model.

Reconstruction of a network model and arrangement of nodes into modules. We focused on a network model describing cellular processes represented by the up-regulated genes in the three groups ('shared', 'FLS-dominant', and 'SM-dominant') shown in **Fig. 1*C***. Among the 1818 up-regulated genes (396 up-regulated genes in RA-FLS, 691 genes in IL1β-stimulated RA-FLS, and 1048 genes in RA-SM), we first selected 357 up-regulated genes that were involved in the 16 cellular processes in **Fig. 1*C***, which can be categorized the following two groups: 1) invasion-related processes, including ECM organization (ECM), regulation of EMT (EMT), WNT signaling (WNT), and cell adhesion and migration (CAM); and 2) inflammation-related processes, including inflammatory cytokines (IC), regulation of cell proliferation (RCP), cytoskeleton organization (CO), complement and coagulation (CC), chemotaxis (CK), JAK-STAT signaling (JS), anti-apoptosis (AA), response to ER-stress (RES), angiogenesis (AG), cytokine production (CP), antigen presentation (AP), and leukocyte activation (LA).

To reconstruct a network model for the 357 genes, we first downloaded all protein-

protein interactions (PPIs) stored in HPRD (17), BioGRID (18), STRING (19), and KEGG (20) and then combined all PPIs from the four databases into one list of PPIs. During this process, we converted protein IDs used in each database into Entrez IDs, converted directed PPIs from the KEGG pathway database into undirected PPIs to be compatible with undirected PPIs obtained from the three databases, and generated a list of non-redundant PPIs by removing redundant PPIs in the four databases. From the combined list of PPIs, we selected the PPIs among the 357 genes. All these procedures were implemented in a MATLAB. We then used Cytoscape version 2.8.2 to display these PPIs for the 357 genes as a network model.

Using the GOBPs (21) of the 357 genes corresponding to the aforementioned 16 cellular processes (**Fig. 1*C***), we arranged the corresponding nodes in the network such that the ones with the same GOBPs were grouped into the same network modules, thereby resulting in 16 modules. Nodes can have multiple GOBPs of the 16 GOBPs. For each of these nodes, we counted the interactors with the multiple GOBPs and then included the node to the modules in which the largest number of its interactors was included.

Knock-down of TWIST1 and POSTN transcripts. RA-FLS were transfected with TWIST1, TGFB1I1, and POSTN siRNAs (Dharmacon, Lafayette, CO) using DharmaFect (Dharmacon, Lafayette, CO). Scrambled RNAs were purchased from Santa Cruz Biotechnology (Santa Cruz, CA).

Real-time PCR. Total RNA was subjected to cDNA synthesis using a High Capacity cDNA RT kit (Applied Biosystems, Foster City, CA), according to the manufacturer's instructions. Quantitative real-time PCR was performed in the CFX96™ Real-Time PCR System (Bio-

Rad, Hercules, CA) using SYBR Premix (Bio-Rad), according to the manufacturer's instructions. GAPDH was used as an internal control for PCR amplification. Transcript levels were calculated relative to controls, and relative fold inductions were calculated by using $2^{-\Delta\Delta Ct}$ algorithm (22). The gene-specific primers used are listed in **Table S4**.

Western blot analysis. Cells were lysed in lysis buffer and insoluble material was removed by centrifugation at 12,000g for 20 minutes at 4°C. Final protein concentrations were determined using the Bradford protein assay (Bio-Rad). Electrophoresis was carried out using sodium dodecyl sulfate-10% polyacrylamide gels electrophoresis (SDS-PAGE), and the resolved proteins were transferred to nitrocellulose membranes. Membranes were incubated with antibodies (Abs) to TWIST1 (Abcam, Cambridge, UK), POSTN (Abcam), and β-actin (Sigma-Aldrich, St Louis, MO). Membranes were then visualized using an enhanced chemiluminescence technique (ECL). Resulting films were scanned and optical densities were quantified using Quantity On 1-D software (Bio-Rad) or ImageJ software (http://rsb.info.nih.gov/ij/index.html). Experiments were repeated three to four times for separate samples.

Cell viability: MTT assay. After knocking down TWIST1, TGFB1I1, and POSTN mRNA, synoviocyte viability was determined by an MTT assay, as described previously (23).

Wound migration assay for synoviocyte. After knocking down POSTN, TWIST1, and TGFB1I1, wound migration of RA-FLS was measured as described previously (12). In brief, RA-FLS plated to confluence on 60-mm culture dishes were wounded with pipette tips and then treated with IL1β in DMEM supplemented with 1% FBS. After 24 to 36 h incubation,

FLS migration was quantified by counting the cells that had moved beyond a reference line. Cell migration was also dynamically assessed by the Cell-IQ (Chip-Man Technologies, Tampere, Finland) over a period of 50 h, and the result images were then analyzed by batch process using the Analyser™ software. Three regions of interest per well per wound edge were chosen for imaging.

Matrigel invasion assay. The BD BioCoat Matrigel Invasion Chamber assay system (Becton Dickinson, Heidelberg, Germany) was used to study FLS invasion, according to the manufacturer's instructions. In brief, 24 h after transfection with siRNA, RA-FLS were allowed to migrate in Matrigel invasion chamber for additional 24 h in the presence of DMEM containing 10% FCS or 10 ng/ml of IL1β in DMEM supplemented with 1% FBS. The non-invading cells were afterward removed by scrubbing with a cotton-tipped swab, and the cells on the lower surface of the membrane were stained with Diff-Quik stain (Baxter Diagnostics, McGaw Park, IL). For quantification, cells were counted in eight random fields.

Determination of FLS migration *in vivo*. RA-FLS ($5X10^5$) were transfected with control siRNA, POSTIN siRNA or TWIST1 siRNA for 24 hours. The FLS were then labeled with 0.2 mg/ml of NEO-STEM™ containing fluorescent dyes of NIR 675 (Biterials, Seoul, Korea) (24), and the labeled cells were injected intra-dermally into the back of athymic nude mice (Jackson Laboratory, Bar Harbor, ME). One day before FLS implantation, skin inflammation was induced by subcutaneously injecting complete Freund’s adjuvant (CFA) into the skin at a fixed distance (1.2 cm) from the injection site for FLS. After 5 days, skin samples were obtained from the FLS-implanted site, CFA-injected site, as well as between the two. Sections were analyzed under the confocal microscopy (Zeiss LSM 510; Carl Zeiss Inc.,

Thornwood, NJ) or subjected to immuno-histochemical staining for HLA class I. For immuno-histochemical staining, tissue sections were blocked with bovine serum albumin (BSA) for 30 minutes at room temperature. Sections were then incubated with Abs to HLA class I (1:100, Abcam) overnight at 4°C. Each slide was washed three times in TBS and incubated with biotinylated anti-mouse IgG (Vector Laboratories, Burlingame, CA) in a humid chamber for 30 minutes. HLA class I-positive cells were detected using peroxidase-conjugated streptavidin (Vector Laboratories) followed by 3'3-diaminobenzidine tetrahydrochloride (DAB; Vector Laboratories). The slides were counterstained with hematoxylin. Whole slide image capture was performed on a Pannoramic MIDI slide scanner (3DHISTECH Ltd., Budapest, Hungary). The number of HLA-class I (+) cells, indicating RA-FLS, was determined by counting positively staining cells in digitalized images covering the entire area of skin.

Statistical analyses. Using normalized intensity values, DEGs from all the four comparisons 1) RA-FLS/OA-FLS, 2) RA-SM/healthy controls, 3) RA-FLS+IL1β/OA-FLS, and 4) RA-FLS+IL1β/OA-FLS+IL1β) were identified using the integrative statistical method previously reported (14). Briefly, for each gene, an adjusted *P*-value was computed by performing a two-tailed T-test and log2 median ratio test using the empirical distributions that were estimated by random permutations of the samples. The two sets of *P*-values from the individual tests were combined to compute the overall *P*-values using Stouffer's method (25). Finally, the DEGs were selected with the ones having 1) $P \leq 0.05$, 2) absolute log2-fold-changes larger than 1.34. To determine the cutoff value of log2-fold-changes, we computed log2-fold-changes of randomly permuted samples, fitted a Gaussian distribution to the random log2-fold-changes, and then calculated 2.5^{th} percentile corresponding to $\alpha = 0.05$ (log2-fold-change

cutoff = 1.34). The DEGs were grouped into eight clusters using hierarchical clustering. The cellular processes represented by the genes in each cluster were identified as the GO biological processes (GOBPs) having $P < 0.1$ (the default cutoff value in the DAVID software) (15).

In the *in vitro* functional experiments, data are expressed as the mean ± standard deviation (SD). Comparisons of the numerical data between groups were performed by the T-test or Mann-Whitney U-test. *P* values less than 0.05 were considered statistically significant.

SI Figures, Tables, Datasets, and Movies

List of Supporting Figures

Fig. S1. Cellular processes enriched by the genes in down-regulated clusters.

Fig. S2. Increased expression of pro-inflammatory genes in RA macrophages. Quantitative real-time PCR assays for a subset of genes representing SM-dominant cellular processes in RA (n=6) and OA macrophages (n=6) freshly isolated from synovial tissues. Relative mRNA expression was calculated by the $2^{-\Delta\Delta Ct}$ algorithm. Results are the mean ± SEM and represent three independent experiments. *, $P < 0.05$.

Fig. S3. Network model describing invasive potential of RA-FLS and inflammatory potential of SM. (***A***) A network model describing the shared, FLS-dominant, and SM-dominant processes in **Figs. 1*C* and 2*B***, which are represented by the 357 up-regulated DEGs in RA-FLS, RA-SM, and IL1β-stimulated RA-FLS. The nodes are arranged into the 16 modules as described in **SI *Materials and Methods***. Node (magenta), boundary (red), and

label colors (blue) represent the DEGs in RA-FLS, IL1β-stimulated RA-FLS, and RA-SM, respectively (*See the node and legend in the bottom*). The modules were named by the corresponding GOBPs and distinguished by dotted lines. (***B***) 3-dimensional conic graphs showing module enrichment scores (MES) representing the contribution of RA-FLS and SM to the individual modules (**Table S2**). The three sets of MES were computed from the comparisons of RA-FLS and OA-FLS (left), RA-FLS+IL1β and unstimulated OA-FLS (middle), and RA-SM and control macrophages (right). The height of circular cones indicates the magnitude of the MES in the corresponding module. The purple cone represents that the *P*-value of MES for the corresponding modules is less than 0.01, while the gray cone represents MES with $P > 0.01$.

Fig. S4. Selection process of key regulators responsible for the migration and invasion of FLS. (**A**) Venn diagram depicting 946 up-regulated genes in either RA-FLS or IL1β-stimulated RA-FLS. (**B**) Selection process of 13 novel regulators out of the 946 up-regulated genes in either RA-FLS or IL1β-stimulated RA-FLS.

Fig. S5. POSTN and TWIST1 control IL1β-induced FLS invasion. (***A* and *B***) Regulation of FLS invasion by POSTN and TWIST1. Twenty four hours after transfection with POSTN siRNA, TWIST1 siRNA, or TGFB1I1 siRNA, RA-FLS were allowed to migrate in Matrigel invasion chamber for additional 24 h in the presence of DMEM containing 10% FCS (***A***) or 10 ng/ml of IL1β (***B***). Invaded cells were stained violet using Diff-Quik kit. Results are the mean ± SEM, and represent three independent experiments. *, $P < 0.05$. (***C*** to ***E***) Reduction of FLS migration *in vivo* by POSTN or TWIST1 siRNA. (***C***) A schematic model of the *in vivo* migration assay. In severe combined immune-deficient (SCID) mice, skin inflammation

was induced by subcutaneously injecting complete Freund's adjuvant (CFA, 120 μg) into site (**a**). One day after the CFA injection, RA-FLS ($5X10^5$) labeled with fluorescent dyes of NIR 675 (NEO-STEM^{TM}) were implanted intra-dermally in site (**c**), which is 1.2 cm apart from site (**a**). After 5 days of the FLS implantation, skin samples were obtained from sites (**a**), (**b**), and (**c**). In the top portion, increased dermal infiltration of inflammatory cells in the CFA-injected site was seen in the hematoxyllin and eosin stain. In the bottom portion, a cluster of RA-FLS (arrowheads) was detected in the skin obtained from site (**a**), as determined by immuno-histochemical staining using anti-HLA class I antibody. (***D***) Confocal microscopic or immuno-histochemical analysis of the skin tissues between FLS implantation and CFA injection site. NIR 675-labeled RA-FLS appear green under the confocal microscopy (left panel). The cells positive for HLA class I, indicating RA-FLS, are shown in brown (right panel). Rectangular areas on the right are magnified to the photographs on the left. Data are the representative photographs of independent experiments performed in more than five skin sections for each mouse. (***E***) Numbers of RA-FLS stained with anti-HLA class I antibody. Cells were manually counted in digitalized images covering the whole area of skin. Values are the mean ± SD of 3 mice per each group. *, $P < 0.0001$ versus control siRNA-transfected FLS.

Fig. S6. Novel regulators for the inflammatory potential newly acquired in RA-FLS by the IL1β stimulation. (*A*) Potential regulators associated with the inflammatory potential newly acquired in RA-FLS by the IL1β stimulation. (***B***) A network model describing regulator-target gene relationships and their associated cellular processes.

List of Supporting Tables

Table S1. Genes included in the network model (**Fig. S3*A***).

Table S2. Module enrichment scores (MES) for the contribution of RA-FLS and RA-SM in each module.

Table S3. 13 candidate genes with gene name, Entrez gene id, and regulation factors.

Table S4. Sequences of gene specific primers used for real-time PCR.

Supporting Dataset (*uploaded separately*)

Dataset S1. Lists of the DEGs in RA-FLS, RA-SM, and IL1β-stimulated RA-FLS. The list of the DEGs from each comparison includes Entrez ID, Gene description, *P*-value, and log2-fold-change.

Supporting Movie (*uploaded separately*)

Movie S1. Real-time dynamics of FLS migration. Confluent cultures of RA-FLS transfected with POSTN siRNA (***A***) or control siRNA (***B***) were scratched, and wound closure was examined over a period of 50 h. Images were taken with Cell-IQ.

SI References

1. Romanos GE, Asnani KP, Hingorani D, & Deshmukh VL (2013) Periostin: Role in formation and maintenance of dental tissues. *J Cell Physiol* (In Press).
2. Elliott CG, Kim SS, & Hamilton DW (2012) Functional significance of periostin in excisional skin repair: is the devil in the detail? *Cell Adh Migr* 6(4):319-326.
3. Naik PK, *et al.* (2012) Periostin promotes fibrosis and predicts progression in patients with idiopathic pulmonary fibrosis. *Am J Physiol Lung Cell Mol Physiol* 303(12):L1046-1056.
4. Morra L & Moch H (2011) Periostin expression and epithelial-mesenchymal transition in cancer: a review and an update. *Virchows Arch* 459(5):465-475.
5. Yan W & Shao R (2006) Transduction of a mesenchyme-specific gene periostin into 293T cells induces cell invasive activity through epithelial-mesenchymal transformation. *J Biol Chem* 281(28):19700-19708.
6. Ontsuka K, *et al.* (2012) Periostin, a matricellular protein, accelerates cutaneous wound repair by activating dermal fibroblasts. *Exp Dermatol* 21(5):331-336.
7. Martin A & Cano A (2010) Tumorigenesis: Twist1 links EMT to self-renewal. *Nat Cell Biol* 12(10):924-925.
8. Lee MP & Yutzey KE (2011) Twist1 directly regulates genes that promote cell proliferation and migration in developing heart valves. *PLoS One* 6(12):e29758.
9. Oshima A, *et al.* (2002) A novel mechanism for the regulation of osteoblast differentiation: transcription of periostin, a member of the fasciclin I family, is regulated by the bHLH transcription factor, twist. *J Cell Biochem* 86(4):792-804.
10. Qin Q, Xu Y, He T, Qin C, & Xu J (2012) Normal and disease-related biological functions of Twist1 and underlying molecular mechanisms. *Cell Res* 22(1):90-106.

11. Yoo SA, *et al.* (2006) Calcineurin is expressed and plays a critical role in inflammatory arthritis. *J Immunol* 177(4):2681-2690.

12. Yoo SA, *et al.* (2012) A novel pathogenic role of the ER chaperone GRP78/BiP in rheumatoid arthritis. *J Exp Med* 209(4):871-886.

13. Bolstad BM, Irizarry RA, Astrand M, & Speed TP (2003) A comparison of normalization methods for high density oligonucleotide array data based on variance and bias. *Bioinformatics* 19(2):185-193.

14. Lee HJ, *et al.* (2010) Direct transfer of alpha-synuclein from neuron to astroglia causes inflammatory responses in synucleinopathies. *J Biol Chem* 285(12):9262-9272.

15. Huang da W, Sherman BT, & Lempicki RA (2009) Systematic and integrative analysis of large gene lists using DAVID bioinformatics resources. *Nat Protoc* 4(1):44-57.

16. You S, *et al.* (2012) A systems approach to rheumatoid arthritis. *PLoS One* 7(12):e51508.

17. Peri S, *et al.* (2004) Human protein reference database as a discovery resource for proteomics. *Nucleic Acids Res* 32(Database issue):D497-501.

18. Stark C, *et al.* (2006) BioGRID: a general repository for interaction datasets. *Nucleic Acids Res* 34(Database issue):D535-539.

19. von Mering C, *et al.* (2003) STRING: a database of predicted functional associations between proteins. *Nucleic Acids Res* 31(1):258-261.

20. Ogata H, *et al.* (1999) KEGG: Kyoto Encyclopedia of Genes and Genomes. *Nucleic Acids Res* 27(1):29-34.

21. Ashburner M, *et al.* (2000) Gene ontology: tool for the unification of biology. The Gene Ontology Consortium. *Nat Genet* 25(1):25-29.

22. Livak KJ & Schmittgen TD (2001) Analysis of relative gene expression data using real-time quantitative PCR and the 2(-Delta Delta C(T)) Method. *Methods* 25(4):402-408.

23. Lee MS, *et al.* (2006) Serum amyloid A binding to formyl peptide receptor-like 1 induces synovial hyperplasia and angiogenesis. *J Immunol* 177(8):5585-5594.

24. Yeum CE, Park EY, Lee SB, Chun HJ, & Chae GT (2013) Quantification of MSCs involved in wound healing: use of SIS to transfer MSCs to wound site and quantification of MSCs involved in skin wound healing. *J Tissue Eng Regen Med* 7(4):279-291.

25. Hwang D, *et al.* (2005) A data integration methodology for systems biology. *Proc Natl Acad Sci U S A* 102(48):17296-17301.

Supporting information Fig. S1

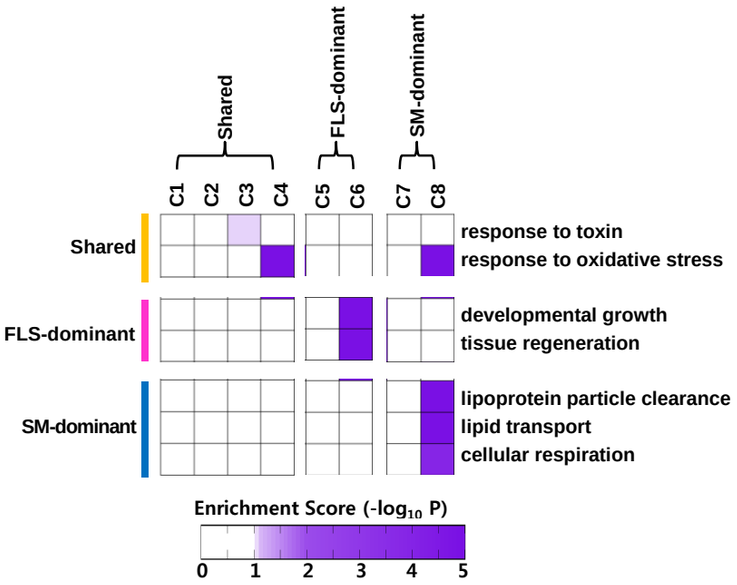

Supporting information Fig. S2

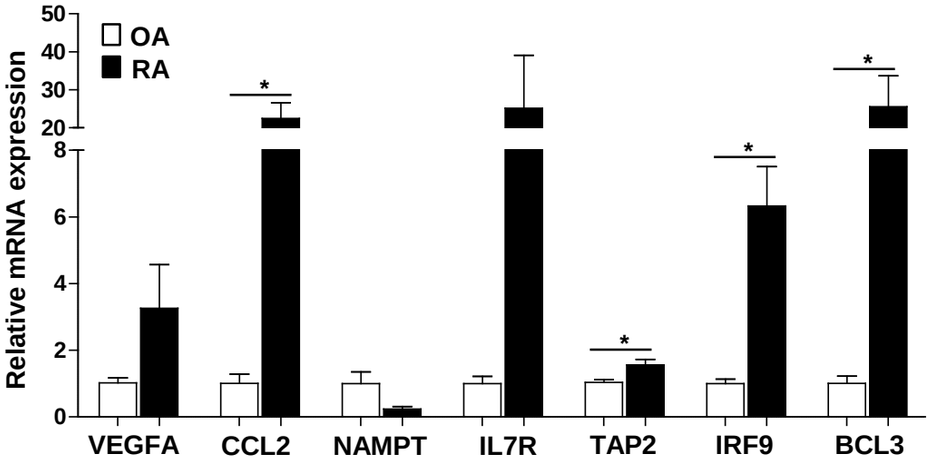

Supporting information Fig. S3

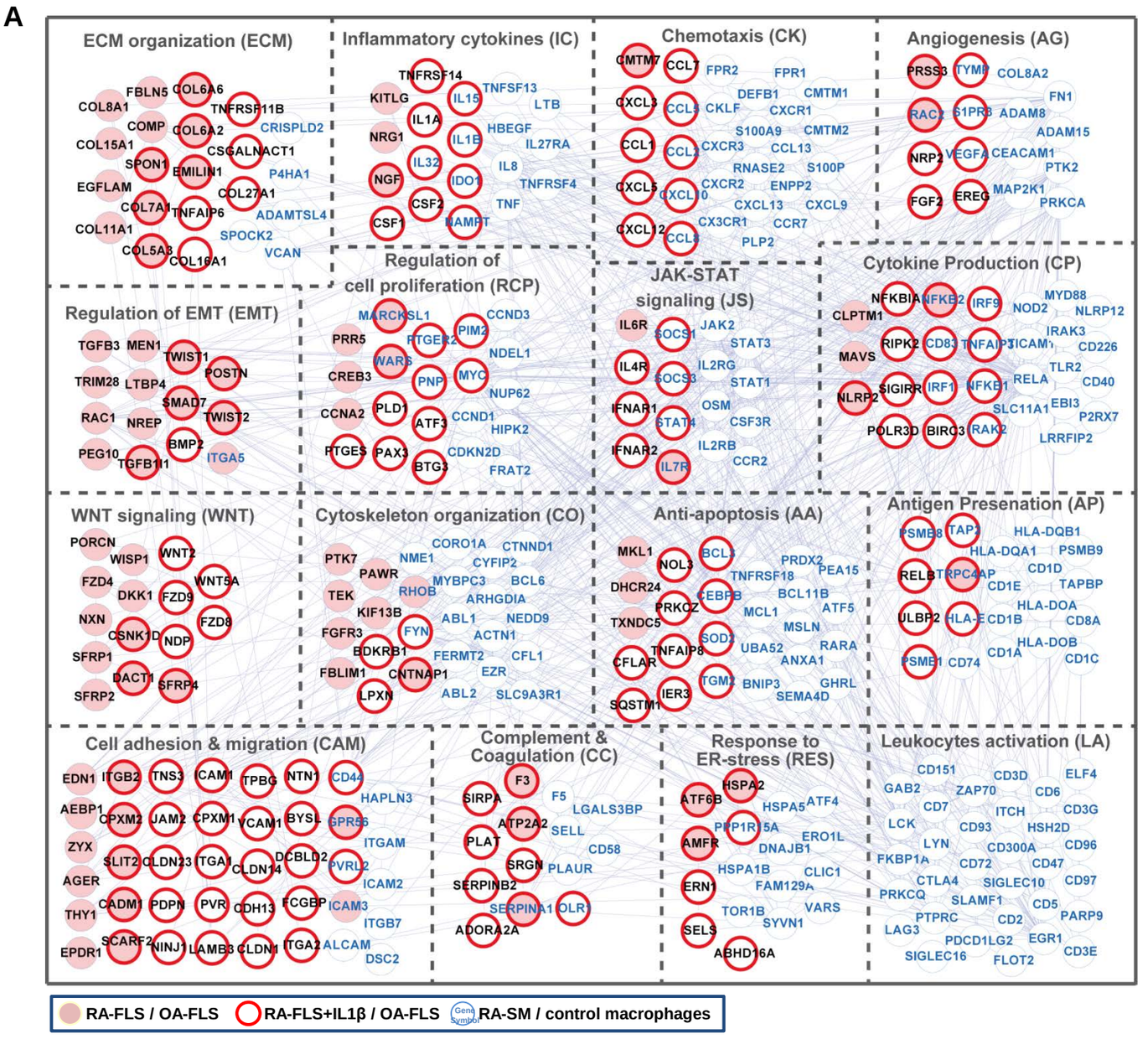

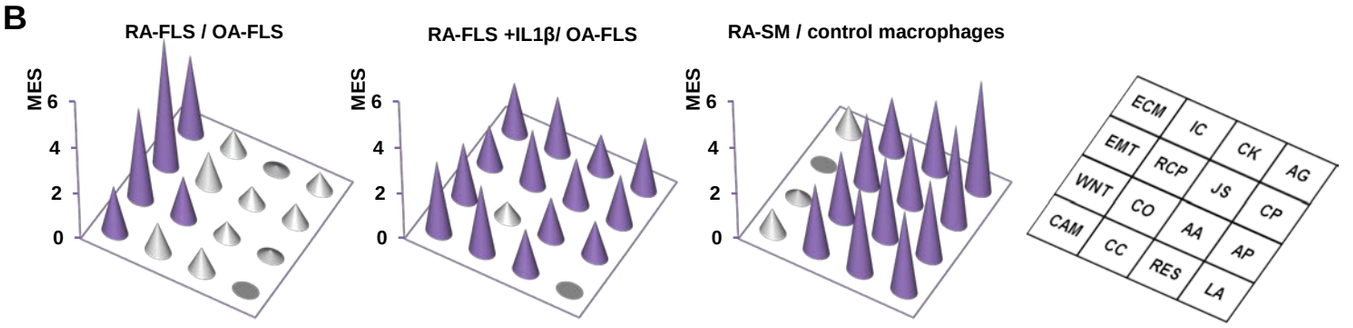

Supporting information Fig. S4

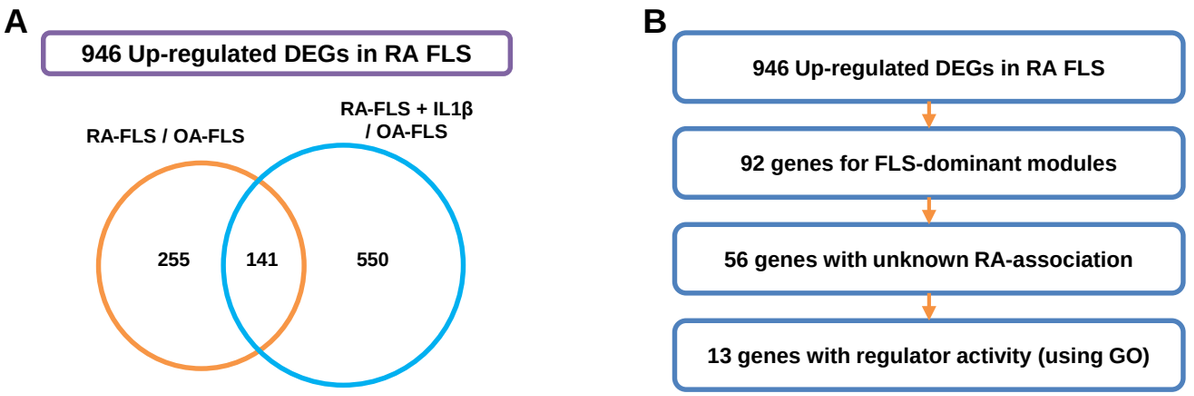

Supporting information Fig. S5

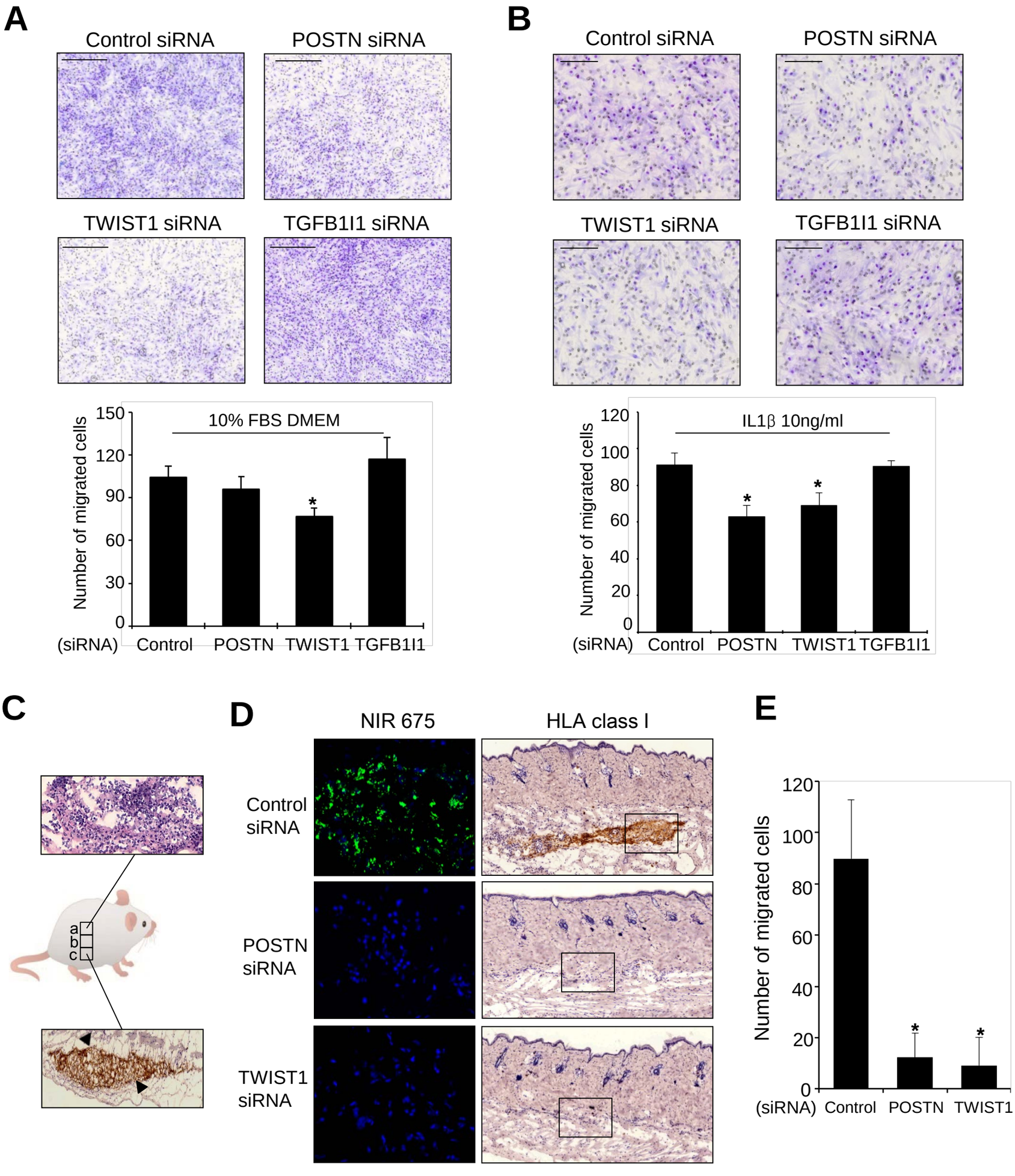

Supporting information Fig. S6

A

Gene Symbol	TF	Signaling
AMFR	-	O
ATF6B	O	O
S1PR3	-	O
FYN	-	O
CXCL3	-	O
IFNAR1	-	O
IFNAR2	-	O
IER3	-	O
SLIT2	-	O
IRF9	O	O
PIM2	-	O
PPP1R15A	-	O
TNFAIP8	-	O
SIGIRR	-	O
TWIST2	O	-

B

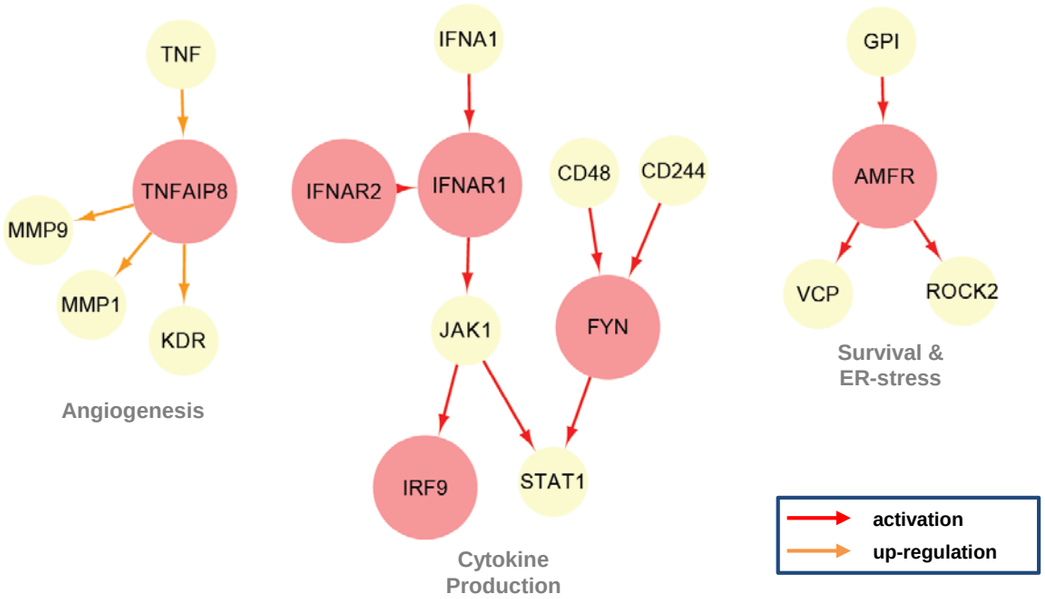

Supporting information Table S1.

	MES Score		
Module name	**RA-FLS / OA-FLS**	**RA-FLS + IL1ß / OA-FLS**	**RA-SM / control macrophages**
ECM organization (ECM)	3.412	2.218	1.046
Regulation of EMT (EMT)	5.572	1.784	0.37
WNT signaling (WNT)	4.024	2.473	0
Cell adhesion & migration (CAM)	2.061	3.167	1.173
Inflammatory cytokines (IC)	0.953	2.441	3.038
Regulation of cell proliferation (RCP)	1.437	2.429	2.978
Cytoskeleton organization (CO)	1.857	0.713	3.145
Complement & coagulation (CC)	1.293	2.981	2.405
Chemotaxis (CK)	0.208	1.599	3.815
JAK-STAT signaling (JS)	0.755	2.029	3.608
Anti-apoptosis (AA)	0.696	1.784	3.145
Response to ER-stress (RES)	1.065	1.91	3.113
Angiogenesis (AG)	0.755	2.319	3.608
Cytokine production (CP)	0.862	2.153	3.436
Antigen presentation (AP)	0.302	1.623	4.329
Luekocytes activation (LA)	0	0	4.81

Supporting information Table S2.

		Differential expression		
Entrez ID	**Gene Symbol**	**RA-FLS / OA-FLS**	**RA-FLS+IL1β / OA-FLS**	**RA-SM / control macrophages**
2921	CXCL3	None	Up-regulated	None
4814	NINJ1	None	Up-regulated	None
5055	SERPINB2	None	Up-regulated	None
8651	SOCS1	None	Up-regulated	Up-regulated
5027	P2RX7	None	None	Up-regulated
8837	CFLAR	None	Up-regulated	None
4790	NFKB1	None	Up-regulated	Up-regulated
6286	S100P	None	None	Up-regulated
2534	FYN	None	Up-regulated	Up-regulated
4739	NEDD9	None	None	Up-regulated
133584	EGFLAM	Up-regulated	None	None
5604	MAP2K1	None	None	Up-regulated
113540	CMTM1	None	None	Up-regulated
64919	BCL11B	None	None	Up-regulated
9308	CD83	None	Up-regulated	Up-regulated
9021	SOCS3	None	Up-regulated	Up-regulated
400709	SIGLEC16	None	None	Up-regulated
5329	PLAUR	None	None	Up-regulated
5033	P4HA1	None	None	Up-regulated
3914	LAMB3	None	Up-regulated	None
1295	COL8A1	Up-regulated	None	None
8325	FZD8	None	Up-regulated	None
3306	HSPA2	Up-regulated	Up-regulated	None
1435	CSF1	None	Up-regulated	None
3552	IL1A	None	Up-regulated	None
3384	ICAM2	None	None	Up-regulated
7422	VEGFA	None	Up-regulated	Up-regulated
5879	RAC1	Up-regulated	None	None
51339	DACT1	Up-regulated	Up-regulated	None
2081	ERN1	None	Up-regulated	None
10135	NAMPT	None	Up-regulated	Up-regulated
23562	CLDN14	None	Up-regulated	None
50509	COL5A3	Up-regulated	Up-regulated	None
64759	TNS3	None	Up-regulated	None
165	AEBP1	Up-regulated	None	None
80380	PDCD1LG2	None	None	Up-regulated
5168	ENPP2	None	None	Up-regulated
55790	CSGALNACT1	None	Up-regulated	None
7412	VCAM1	None	Up-regulated	None
910	CD1B	None	None	Up-regulated
9289	GPR56	Up-regulated	Up-regulated	Up-regulated
1192	CLIC1	None	None	Up-regulated
6556	SLC11A1	None	None	Up-regulated
5588	PRKCQ	None	None	Up-regulated
11040	PIM2	None	Up-regulated	Up-regulated
8996	NOL3	None	Up-regulated	None
117581	TWIST2	Up-regulated	Up-regulated	None
6504	SLAMF1	None	None	Up-regulated
3575	IL7R	Up-regulated	Up-regulated	Up-regulated
7791	ZYX	Up-regulated	None	None

Table continues on the following page.

		Differential expression		
Entrez ID	**Gene Symbol**	**RA-FLS / OA-FLS**	**RA-FLS+IL1β / OA-FLS**	**RA-SM / control macrophages**
6354	CCL7	None	Up-regulated	None
1231	CCR2	None	None	Up-regulated
5754	PTK7	Up-regulated	None	None
6355	CCL8	None	Up-regulated	Up-regulated
7311	UBA52	None	None	Up-regulated
8425	LTBP4	Up-regulated	None	None
7130	TNFAIP6	None	Up-regulated	None
7052	TGM2	None	Up-regulated	Up-regulated
10631	POSTN	Up-regulated	Up-regulated	None
9404	LPXN	None	Up-regulated	None
976	CD97	None	None	Up-regulated
3717	JAK2	None	None	Up-regulated
6346	CCL1	None	Up-regulated	None
3133	HLA-E	None	Up-regulated	Up-regulated
5698	PSMB9	None	None	Up-regulated
3695	ITGB7	None	None	Up-regulated
909	CD1A	None	None	Up-regulated
5077	PAX3	None	Up-regulated	None
916	CD3E	None	None	Up-regulated
101	ADAM8	None	None	Up-regulated
5646	PRSS3	Up-regulated	Up-regulated	None
1437	CSF2	None	Up-regulated	None
3112	HLA-DOB	None	None	Up-regulated
5880	RAC2	Up-regulated	Up-regulated	Up-regulated
3689	ITGB2	Up-regulated	Up-regulated	None
7001	PRDX2	None	None	Up-regulated
3455	IFNAR2	None	Up-regulated	None
1032	CDKN2D	None	None	Up-regulated
5817	PVR	None	Up-regulated	None
23303	KIF13B	Up-regulated	None	None
3553	IL1B	None	Up-regulated	Up-regulated
9423	NTN1	None	Up-regulated	None
5590	PRKCZ	None	Up-regulated	None
54749	EPDR1	Up-regulated	None	None
22943	DKK1	Up-regulated	None	None
55655	NLRP2	Up-regulated	Up-regulated	None
64359	NXN	Up-regulated	None	None
3672	ITGA1	None	Up-regulated	None
10666	CD226	None	None	Up-regulated
3111	HLA-DOA	None	None	Up-regulated
2152	F3	Up-regulated	Up-regulated	None
7535	ZAP70	None	None	Up-regulated
1072	CFL1	None	None	Up-regulated
3385	ICAM3	Up-regulated	None	Up-regulated
10516	FBLN5	Up-regulated	None	None
7097	TLR2	None	None	Up-regulated
1051	CEBPB	None	Up-regulated	Up-regulated
9536	PTGES	None	Up-regulated	None
388	RHOB	Up-regulated	None	Up-regulated
958	CD40	None	None	Up-regulated

Table continues on the following page.

		Differential expression		
Entrez ID	**Gene Symbol**	**RA-FLS / OA-FLS**	**RA-FLS+IL1β / OA-FLS**	**RA-SM / control macrophages**
10232	MSLN	None	None	Up-regulated
89790	SIGLEC10	None	None	Up-regulated
58494	JAM2	None	Up-regulated	None
4609	MYC	None	Up-regulated	Up-regulated
923	CD6	None	None	Up-regulated
54751	FBLIM1	Up-regulated	None	None
3560	IL2RB	None	None	Up-regulated
3932	LCK	None	None	Up-regulated
2261	FGFR3	Up-regulated	None	None
3627	CXCL10	None	Up-regulated	Up-regulated
5337	PLD1	None	Up-regulated	None
5819	PVRL2	None	Up-regulated	Up-regulated
56265	CPXM1	None	Up-regulated	None
11117	EMILIN1	Up-regulated	Up-regulated	None
1453	CSNK1D	Up-regulated	Up-regulated	None
3304	HSPA1B	None	None	Up-regulated
6352	CCL5	None	Up-regulated	Up-regulated
4615	MYD88	None	None	Up-regulated
8741	TNFSF13	None	None	Up-regulated
10225	CD96	None	None	Up-regulated
4221	MEN1	Up-regulated	None	None
2000	ELF4	None	None	Up-regulated
1839	HBEGF	None	None	Up-regulated
488	ATP2A2	Up-regulated	Up-regulated	None
914	CD2	None	None	Up-regulated
705	BYSL	None	Up-regulated	None
2358	FPR2	None	None	Up-regulated
28996	HIPK2	None	None	Up-regulated
9353	SLIT2	Up-regulated	Up-regulated	None
6422	SFRP1	Up-regulated	None	None
23705	CADM1	Up-regulated	Up-regulated	None
3566	IL4R	None	Up-regulated	None
2280	FKBP1A	None	None	Up-regulated
1209	CLPTM1	Up-regulated	None	None
8828	NRP2	None	Up-regulated	None
84447	SYVN1	None	None	Up-regulated
11151	CORO1A	None	None	Up-regulated
148022	TICAM1	None	None	Up-regulated
26999	CYFIP2	None	None	Up-regulated
5788	PTPRC	None	None	Up-regulated
83737	ITCH	None	None	Up-regulated
9209	LRRFIP2	None	None	Up-regulated
9846	GAB2	None	None	Up-regulated
83666	PARP9	None	None	Up-regulated
4860	PNP	None	Up-regulated	Up-regulated
4607	MYBPC3	None	None	Up-regulated
9076	CLDN1	None	Up-regulated	None
59307	SIGIRR	None	Up-regulated	None
7070	THY1	Up-regulated	None	None
1524	CX3CR1	None	None	Up-regulated

Table continues on the following page.

		Differential expression		
Entrez ID	**Gene Symbol**	**RA-FLS / OA-FLS**	**RA-FLS+IL1β / OA-FLS**	**RA-SM / control macrophages**
912	CD1D	None	None	Up-regulated
1824	DSC2	None	None	Up-regulated
2069	EREG	None	Up-regulated	None
604	BCL6	None	None	Up-regulated
9235	IL32	None	Up-regulated	Up-regulated
3561	IL2RG	None	None	Up-regulated
6891	TAP2	None	Up-regulated	Up-regulated
5327	PLAT	None	Up-regulated	None
4170	MCL1	None	None	Up-regulated
6402	SELL	None	None	Up-regulated
468	ATF4	None	None	Up-regulated
6648	SOD2	None	Up-regulated	Up-regulated
3678	ITGA5	Up-regulated	None	Up-regulated
1292	COL6A2	Up-regulated	Up-regulated	None
1462	VCAN	None	None	Up-regulated
11213	IRAK3	None	None	Up-regulated
26133	TRPC4AP	Up-regulated	Up-regulated	Up-regulated
971	CD72	None	None	Up-regulated
6424	SFRP4	Up-regulated	Up-regulated	None
6892	TAPBP	None	None	Up-regulated
1906	EDN1	Up-regulated	None	None
112616	CMTM7	Up-regulated	Up-regulated	None
146225	CMTM2	None	None	Up-regulated
890	CCNA2	Up-regulated	None	None
1441	CSF3R	None	None	Up-regulated
1311	COMP	Up-regulated	None	None
83716	CRISPLD2	None	None	Up-regulated
4693	NDP	None	Up-regulated	None
2247	FGF2	None	Up-regulated	None
5696	PSMB8	None	Up-regulated	Up-regulated
5747	PTK2	None	None	Up-regulated
10950	BTG3	None	Up-regulated	None
1012	CDH13	None	Up-regulated	None
6423	SFRP2	Up-regulated	None	None
30001	ERO1L	None	None	Up-regulated
23401	FRAT2	None	None	Up-regulated
8870	IER3	None	Up-regulated	None
4254	KITLG	Up-regulated	None	None
54507	ADAMTSL4	None	None	Up-regulated
3684	ITGAM	None	None	Up-regulated
960	CD44	None	Up-regulated	Up-regulated
965	CD58	None	None	Up-regulated
8878	SQSTM1	None	Up-regulated	None
595	CCND1	None	None	Up-regulated
602	BCL3	None	Up-regulated	Up-regulated
913	CD1E	None	None	Up-regulated
140885	SIRPA	None	Up-regulated	None
3959	LGALS3BP	None	None	Up-regulated
977	CD151	None	None	Up-regulated
1301	COL11A1	Up-regulated	None	None

Table continues on the following page.

		Differential expression		
Entrez ID	**Gene Symbol**	**RA-FLS / OA-FLS**	**RA-FLS+IL1β / OA-FLS**	**RA-SM / control macrophages**
7041	TGFB1I1	Up-regulated	Up-regulated	None
25	ABL1	None	None	Up-regulated
135	ADORA2A	None	Up-regulated	None
131566	DCBLD2	None	Up-regulated	None
7920	ABHD16A	None	Up-regulated	None
6387	CXCL12	None	Up-regulated	None
131873	COL6A6	Up-regulated	Up-regulated	None
9315	NREP	Up-regulated	None	None
664	BNIP3	None	None	Up-regulated
7124	TNF	None	None	Up-regulated
3117	HLA-DQA1	None	None	Up-regulated
51192	CKLF	None	None	Up-regulated
4067	LYN	None	None	Up-regulated
396	ARHGDIA	None	None	Up-regulated
55615	PRR5	Up-regulated	None	None
3576	IL8	None	None	Up-regulated
4791	NFKB2	Up-regulated	Up-regulated	Up-regulated
1493	CTLA4	None	None	Up-regulated
915	CD3D	None	None	Up-regulated
1307	COL16A1	None	Up-regulated	None
650	BMP2	None	Up-regulated	None
3084	NRG1	Up-regulated	None	None
1236	CCR7	None	None	Up-regulated
4982	TNFRSF11B	None	Up-regulated	None
116496	FAM129A	None	None	Up-regulated
4283	CXCL9	None	None	Up-regulated
23089	PEG10	Up-regulated	None	None
2319	FLOT2	None	None	Up-regulated
5720	PSME1	None	Up-regulated	Up-regulated
65108	MARCKSL1	Up-regulated	Up-regulated	Up-regulated
6775	STAT4	None	Up-regulated	Up-regulated
3600	IL15	None	Up-regulated	Up-regulated
924	CD7	None	None	Up-regulated
972	CD74	None	None	Up-regulated
8751	ADAM15	None	None	Up-regulated
8322	FZD4	Up-regulated	None	None
3570	IL6R	Up-regulated	None	None
4092	SMAD7	Up-regulated	Up-regulated	None
119587	CPXM2	Up-regulated	Up-regulated	None
7128	TNFAIP3	None	Up-regulated	Up-regulated
57506	MAVS	Up-regulated	None	None
81565	NDEL1	None	None	Up-regulated
10563	CXCL13	None	None	Up-regulated
64840	PORCN	Up-regulated	None	None
1958	EGR1	None	None	Up-regulated
7291	TWIST1	Up-regulated	Up-regulated	None
9466	IL27RA	None	None	Up-regulated
3620	IDO1	None	Up-regulated	Up-regulated
1903	S1PR3	None	Up-regulated	Up-regulated
27	ABL2	None	None	Up-regulated

Table continues on the following page.

		Differential expression		
Entrez ID	**Gene Symbol**	**RA-FLS / OA-FLS**	**RA-FLS+IL1β / OA-FLS**	**RA-SM / control macrophages**
5732	PTGER2	None	Up-regulated	Up-regulated
27348	TOR1B	None	None	Up-regulated
3577	CXCR1	None	None	Up-regulated
1388	ATF6B	Up-regulated	Up-regulated	None
896	CCND3	None	None	Up-regulated
330	BIRC3	None	Up-regulated	None
11314	CD300A	None	None	Up-regulated
6280	S100A9	None	None	Up-regulated
10979	FERMT2	None	None	Up-regulated
1500	CTNND1	None	None	Up-regulated
3902	LAG3	None	None	Up-regulated
5970	RELA	None	None	Up-regulated
3673	ITGA2	None	Up-regulated	None
10418	SPON1	Up-regulated	Up-regulated	None
3579	CXCR2	None	None	Up-regulated
10155	TRIM28	Up-regulated	None	None
1294	COL7A1	Up-regulated	Up-regulated	None
85301	COL27A1	None	Up-regulated	None
5265	SERPINA1	Up-regulated	Up-regulated	Up-regulated
7407	VARS	None	None	Up-regulated
8764	TNFRSF14	None	Up-regulated	None
5008	OSM	None	None	Up-regulated
7293	TNFRSF4	None	None	Up-regulated
1306	COL15A1	Up-regulated	None	None
2335	FN1	None	None	Up-regulated
80328	ULBP2	None	Up-regulated	None
7474	WNT5A	None	Up-regulated	None
1672	DEFB1	None	None	Up-regulated
921	CD5	None	None	Up-regulated
267	AMFR	Up-regulated	Up-regulated	None
6774	STAT3	None	None	Up-regulated
8506	CNTNAP1	Up-regulated	Up-regulated	None
6036	RNASE2	None	None	Up-regulated
917	CD3G	None	None	Up-regulated
10148	EBI3	None	None	Up-regulated
145864	HAPLN3	None	None	Up-regulated
10507	SEMA4D	None	None	Up-regulated
23645	PPP1R15A	None	Up-regulated	Up-regulated
5355	PLP2	None	None	Up-regulated
22918	CD93	None	None	Up-regulated
3119	HLA-DQB1	None	None	Up-regulated
961	CD47	None	None	Up-regulated
137075	CLDN23	None	Up-regulated	None
4803	NGF	Up-regulated	Up-regulated	None
5578	PRKCA	None	None	Up-regulated
8840	WISP1	Up-regulated	None	None
1296	COL8A2	None	None	Up-regulated
2833	CXCR3	None	None	Up-regulated
8682	PEA15	None	None	Up-regulated
214	ALCAM	None	None	Up-regulated

Table continues on the following page.

		Differential expression		
Entrez ID	**Gene Symbol**	**RA-FLS / OA-FLS**	**RA-FLS+IL1β / OA-FLS**	**RA-SM / control macrophages**
3309	HSPA5	None	None	Up-regulated
55829	SELS	None	Up-regulated	None
3454	IFNAR1	None	Up-regulated	None
5914	RARA	None	None	Up-regulated
91179	SCARF2	Up-regulated	Up-regulated	None
6772	STAT1	None	None	Up-regulated
25816	TNFAIP8	None	Up-regulated	None
7453	WARS	Up-regulated	Up-regulated	Up-regulated
4830	NME1	None	None	Up-regulated
10630	PDPN	None	Up-regulated	None
4792	NFKBIA	None	Up-regulated	None
7010	TEK	Up-regulated	None	None
3656	IRAK2	None	Up-regulated	Up-regulated
634	CEACAM1	None	None	Up-regulated
9368	SLC9A3R1	None	None	Up-regulated
301	ANXA1	None	None	Up-regulated
5971	RELB	None	Up-regulated	None
2153	F5	None	None	Up-regulated
10379	IRF9	None	Up-regulated	Up-regulated
661	POLR3D	None	Up-regulated	None
177	AGER	Up-regulated	None	None
51738	GHRL	None	None	Up-regulated
91662	NLRP12	None	None	Up-regulated
7043	TGFB3	Up-regulated	None	None
22809	ATF5	None	None	Up-regulated
8767	RIPK2	None	Up-regulated	None
6357	CCL13	None	None	Up-regulated
1890	TYMP	None	Up-regulated	Up-regulated
3659	IRF1	None	Up-regulated	Up-regulated
2357	FPR1	None	None	Up-regulated
1718	DHCR24	Up-regulated	None	None
3337	DNAJB1	None	None	Up-regulated
623	BDKRB1	None	Up-regulated	None
4050	LTB	None	None	Up-regulated
467	ATF3	None	Up-regulated	None
10488	CREB3	Up-regulated	None	None
8857	FCGBP	None	Up-regulated	None
57591	MKL1	Up-regulated	None	None
8326	FZD9	None	Up-regulated	None
9806	SPOCK2	None	None	Up-regulated
6374	CXCL5	None	Up-regulated	None
7430	EZR	None	None	Up-regulated
81567	TXNDC5	Up-regulated	None	None
64127	NOD2	None	None	Up-regulated
23636	NUP62	None	None	Up-regulated
7162	TPBG	None	Up-regulated	None
3383	ICAM1	None	Up-regulated	None
4973	OLR1	None	Up-regulated	Up-regulated
5552	SRGN	None	Up-regulated	None
911	CD1C	None	None	Up-regulated

Table continues on the following page.

		Differential expression		
Entrez ID	**Gene Symbol**	**RA-FLS / OA-FLS**	**RA-FLS+IL1β / OA-FLS**	**RA-SM / control macrophages**
925	CD8A	None	None	Up-regulated
5074	PAWR	Up-regulated	None	None
8784	TNFRSF18	None	None	Up-regulated
87	ACTN1	None	None	Up-regulated
84941	HSH2D	None	None	Up-regulated
6347	CCL2	None	Up-regulated	Up-regulated
7472	WNT2	None	Up-regulated	None

Supporting information Table S3.

Protein 1	Entrez ID	Interaction	Protein 2	Entrez ID	Evidence (PubMed ID)
TWIST1	7291	up-regulation	TIMP1	7076	19513566
TWIST1	7291	inhibition	TP53	7157	18504427
TWIST1	7291	up-regulation	FN1	2335	17512904
TWIST1	7291	up-regulation	CDH2	1000	17512904
TWIST1	7291	down-regulation	CDH1	999	20025748
TGFB1I1	7041	up-regulation	TGFB1	7040	17671518
SMAD7	4092	up-regulation	TGFB1I1	7041	18762808
TGFB1	7040	activation	SMAD7	4092	18762808
POSTN	10631	activation	TNC	3371	19887451
TAB1	10454	activation	MAP3K7	6885	19578758
POSTN	10631	activation	KDR	3791	15082792
POSTN	10631	activation	MAP3K7	6885	19578758
POSTN	10631	activation	AKT1	207	19328625
POSTN	10631	activation	TAB1	10454	19578758
TGFB1I1	7041	up-regulation	FOS	2353	12445807
TWIST1	7291	up-regulation	POSTN	10631	12210745
TGFB1	7040	up-regulation	POSTN	10631	20660732
STAT3	6774	up-regulation	TWIST1	7291	18353781
POSTN	10631	activation	KDR	3791	15082792
TNF	7124	up-regulation	TGFB1I1	7041	11489729
TWIST1	7291	up-regulation	TNF	7124	20007935
TWIST1	7291	up-regulation	IL6	3569	20007935
TWIST1	7291	up-regulation	CCL2	6347	20007935
TGFB1	7040	activation	TWIST1	7291	17684115
TGFB1	7040	activation	CTNNB1	1499	17684115
TGFB1	7040	up-regulation	ACTA2	59	18401422
TWIST1	7291	up-regulation	CDH11	1009	22242143
WNT1	7471	activation	TWIST1	7291	12702582
POSTN	10631	up-regulation	ACTA2	59	19619531
WNT1	7471	activation	CTNNB1	1499	12702582

Table continues on the following page.

Protein 1	Entrez ID	Interaction	Protein 2	Entrez ID	Evidence (PubMed ID)
TRIM28	10155	activation	ZNF74	7625	12684500
TRIM28	10155	activation	NR3C1	2908	9742105
TRIM28	10155	inhibition	TP53	7157	16107876
TRIM28	10155	activation	STAT1	6772	18381204
TRIM28	10155	inhibition	E2F1	1869	17704056
TWIST2	117581	down-regulation	CD7	924	19937140
TWIST2	117581	inhibition	MYEF2	50804	11809751
MEN1	4221	activation	FANCD2	2177	12874027
MEN1	4221	inhibition	PRL	5617	12459032
MEN1	4221	activation	CEBPB	1051	19074834
MEN1	4221	down-regulation	TERT	7015	18636154
MEN1	4221	inhibition	JUND	3727	9989505
AEBP1	165	activation	PPARG	5468	20419060
AEBP1	165	activation	NR1H3	10062	20419060
AEBP1	165	activation	MAPK1	5594	17299101
AEBP1	165	activation	MAPK3	5595	17299101
COL15A1	1306	activation	COL18A1	80781	23621901
CSNK1D	1453	activation	CTNNB1	1499	11818547
CSNK1D	1453	activation	DVL1	1855	11818547
CSNK1D	1453	activation	AXIN1	8312	11818547
CSNK1D	1453	activation	APC	324	11818547
ZYX	7791	activation	VASP	7408	7644520
ZYX	7791	activation	ACTN1	87	10613911
WISP1	8840	up-regulation	VCAM1	7412	23313051
WISP1	8840	up-regulation	MMP2	4313	21453685
GPR56	9289	activation	TGM2	7052	16757564

Supporting information Table S4.

Symbol	Forward	Reverse	Sequence Reference
TWIST1	ATCAAACTGGCCTGCAAAAC	TGCATTTTACCATGGGTCCT	NM_000474.3
TGFB1I1	CTTGCAATTCCAGCGAATC	AGAGGTGGAATGCGTGTGTT	NM_015927.3
POSTN	GCAGACACACCTGTTGGAAA	GTCACGGGGATTTCTTTGAA	NM_006475.1
CSNK1D	CCCATGGATGCTTTCTCAAT	GGGTCCAGCAACAAAGAAAA	NM_001893.3
SMAD7	AGCTGCAGATGGATGTTTCC	TCTTTCAGGGTTTGGGAATG	NM_005904.2
VEGFA	AGTTTTGGGAACACCGACAA	AAGCACAGCAATGTCCTGAA	NM_001025367.1
CCL2	GCTGAGACTAACCCAGAAACATC	GGAATGAAGGTGGCTGCTAT	NM_002982.3
NAMPT	GCCAAATGAGAATCGCAAAG	ATGCAAGGCACACTCCTTTT	NM_005746.2
IL7R	GGAGCCAATGACTTTGTGGT	TCACATGCGTCCATTTGTTT	NM_002185.2
IRF9	CATGCAGAACTGCACACTCA	GCTGCTCCCAATGTCTGAAT	NM_006084.4
TAP2	TCTGGGAACCACAGATGTCA	AAGCGACAAGAAGGGGAAAT	NM_018833.2
BCL3	GTGAACGCGCAAATGTACTC	TCGTTGTGGCAGTTCTTGAG	NM_005178.2
TNF	AAGAGAATTGGGGGCTTAGG	AGGCCCCAGTTTGAATTCTT	NM_000594.2
CDH11	GTGACCCTGAGAAGGCAAAA	GATTCTGGAGGGTGGCAATA	NM_001797.2
ACTA2	TCCTCATCCTCCCTTGAGAA	ATGAAGGATGGCTGGAACAG	NM_001613.1